Materials for life sciences

Focusing and rotating magnetic nanoparticle clusters for fast ablation of thrombus

Qian Li[1,*] , Zhen Lu[2], and Xiaojun Liu[3]

[1] *School of Mechanical Engineering, University of Shanghai for Science and Technology, Shanghai, China*
[2] *College of Computer Science and Technology, Shanghai University of Electric Power, Shanghai, China*
[3] *State Key Laboratory of Digital Manufacturing Equipment and Technology, Huazhong University of Science and Technology, Wuhan, China*

ABSTRACT

Magnetic nanoparticles (MNPs)-mediated drug delivery is considered as a promising method of overcoming comprehensive complications induced by traditional thrombotic or surgery therapies to treat life-threatening thrombus disease. In this study, a novel strategy of combining focusing and rotating MNPs clusters at the targeted site and finally breaking into pieces controlled by a three-dimensional (3D) alternating magnetic field is investigated for further accelerating thrombolysis numerically and experimentally. By applying alternating currents into a group of 3D magnetic coils, the primarily dispersed MNPs were motivated to aggregate into clusters and move toward to an expected position. During the process, the rotation of MNPs induced a strong vortex around them, which drove the urokinase molecular to fast diffuse to the thrombus. In vitro thrombolysis results display that manipulation of MNPs could effectively improve the thrombolysis to twice as much of the pure thrombotic urokinase. To reduce the risk of blocking the microvessels by the large clusters after thrombolysis, the clusters were controlled to break up by improving the frequency of the alternating magnetic field. The theoretical and numerical analysis of the influence of motion of NPs on the fluid was carried out to throw light upon the basis and showed good consistency with the experimental results. Thus, the rotating and focusing of the MNPs by magnetic field could be a promising alternative for the promotion of the thrombolysis rate in future application.

Handling Editor: Dale Huber.

Address correspondence to E-mail: LQ9365@sina.com

GRAPHICAL ABSTRACT
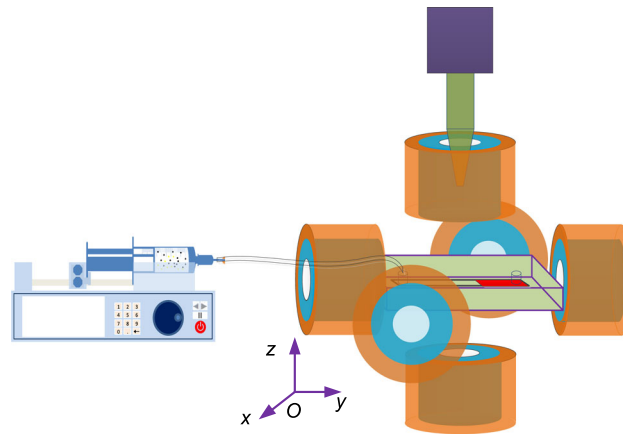
Introduction

Cardiovascular ischemia heart disease and stroke have been the top two diseases that threaten the life health of people all over the world according to the WHO in 2019 [1]. Thrombi were considered as an important underlying cause in these leading fatal diseases by narrowing or occluding the bloodstream and make people death [2, 3]. Traditional systemic thrombolysis through thrombotic infusion, such as urokinase (UK) [4] and streptokinase (SK) [5, 6], is easy to induce hemorrhage complications. Especially for those with acute stroke, therapy at high risk seems to be unavoidable because of injecting large dose of thrombotic in a short time [7, 8]. Nevertheless, looking for alternatives to accelerate thrombolysis while reducing the dosage has still been in efforts during the past decades [9–11].

As an emerging form of therapy, nanomedicine focused on drug delivery and reduction of the side effects induced by the common medical methods [12–15]. By conjugating thrombotic with the carriers or enclosing the drug into polymers [16, 17], the drug could keep its activity for a long time during the circulation. However, the long-time passive transportation and slow-release from the polymers when reaching the destination would conversely decrease the thrombolysis rate. Currently, Fe_3O_4 MNPs-mediated nanodrugs aroused researchers' great interests

for their ability to be non-contact guided to the specific site with magnetic field, which shortened the circulation time in the blood flow [18–20]. Recently, many in vitro thrombolysis experiments were carried out in mimic circulation vessels where permanent magnets could be placed closely to the targets [14, 21, 22]. However, such installments and controlling ways might not be applicable to the in vivo deep vein thrombosis, where thrombi stayed far from the epidermis. This attributes to facts that a single permanent magnet could not retain a distanced objective stably for the rapid decay of magnetic strength as the increasing distance [23, 24]. As a consequence, transporting drug-loaded MNPs to the thrombus target still remained challenging in current.

Meanwhile, what it comes to the design and motion control of the MNPs for drug delivery determines the efficiency in accelerating the thrombolysis. Preparing stable and high-dose magnetic thrombotic has been widely researched before, including our way of bounding the urokinase on the MNPs surface-modified with Poly(maleic anhydride-alt-1-octadecene) [25]. Translation and rotation are two common behaviors of MNPs under the manipulation of the magnetic field. However, in the majority of previous thrombolysis experiments, accumulating MNPs through translation controlled by static magnetic field is the main alternative, which limits the scope of application. The rotation could enhance the mixing effect by inducing the vortex of in

the solvent, while this action has not been being applied in the clinical therapy.

In this study, a novel method of promoting thrombolysis rate through combining translation and rotation of MNPs clusters was researched. Firstly, the theoretical model of MNPs' translation and rotation under magnetic field was constructed and simulated with MATLAB, respectively. Monte Carlo method combined with cluster-moving was adopted to throw light upon the mechanism of forming large clusters from single MNPs. Meanwhile, breaking up the MNPs clusters by changing the magnetic frequency is put forward and researched. Secondly, focusing MNPs in depth with a 3D alternating magnetic field produced by a group of hollow magnetic coils is analyzed and simulated with the combination of COMSOL and MATLAB. Thirdly, a group of 3-D electromagnetic coils is designed for a high magnetic gradient by using particle swarm optimization (PSO) algorithm. Finally, rotational magnetic clusters are analyzed for the diffusion enhancing for the vortex induced by the motion. Thrombolysis experiments by translating and rotating MNPs controlled by the alternating magnetic field generated by the designed group of electromagnetic coils are analyzed and carried out in a microfluidic channel. The results show that the thrombolysis rate can be improved to two or more times than the pure urokinase. Meanwhile, the cluster redispersion experiments are performed and observed by improving the frequency current into the coils, which corresponds to the frequency of the alternating magnetic field in the space. Therefore, it is expected to combine the focusing actuation and rotation motion of the NPs to enhance the thrombolysis while reducing the dosage use. The redispersion test will help promote the feasibility by minimizing the risk of occluding the microvessel in vivo in future.

Materials and methods

Materials

The urokinase and other materials for the synthesis of MNPs and were purchased from Macklin, Shanghai, China, and J&K Scientific Ltd., Beijing, China, and synthesis process can be found in our former published paper [26].

MNPs translation and cluster formation

When a NP is positioned at the magnetic field, it will be magnetized and obtain magnetic momentum. The magnetic potential between two MNPs can be as:

$$U_m = \frac{\mu_0}{4\pi r_{ij}^3}[\vec{m}_i \cdot \vec{m}_j - 3(\vec{m}_i \cdot \vec{r}_{ij})(\vec{m}_j \cdot \vec{r}_{ij})]$$

where μ_0 is the vacuum permeability, m_i and m_j are the magnetic moment of the MNPs, $\vec{r}_{ij}$ represents the displacement vector between the two MNPs i and j. The summation of the potential between any two MNPs will be the total energy of the system.

The MNPs system is always seeking for a equilibrium by decreasing the energy of the system [26]. The formation of magnetic clusters was simulated with MATLAB in a two-dimensional system. Cluster-moving method was combined with the Monte Carlo Method for the motion simulation. Simulation was carried out by applying 500 MNPs in a 5 μm × 5 μm plane area. The MNPs with radius of 50 nm were randomly generated in such an area. A uniform magnetic field 0.5 T in the vertical axis was applied to magnetize the NPs. Choose a random NP and then give it a motion displacement in any direction. The system energy relative to this NP was calculated to make a comparison with the energy before motion. If the energy increased, the NPs would return the original place; otherwise, the new position of the NPs was accepted and the next random NPs would be chosen for another movement. In order to improve the simulation efficiency, the clusters are chosen to move every other two steps of all the MNPs motion. To avoid the overlapping of the NPs, the clusters will return to the original place once the distance between the NPs in and out of the clusters is less than a specific value, which is set as the cut-off radius. The simulation system based on Monte Carlo method is shown in Fig. 1. After 500 steps of simulation, the MNPs in the system have aggregated into rod-like clusters. From the statistics, there are 21 chains formed in the system. The largest number of particles in a chain is 20. There are no single MNPs in the system. Meanwhile, the total energy of the system decreases from 10 to -5×10^{-18} J. This is coincident with the theoretical analysis that the MNPs aggregate as the decrease of the energy.

Furthermore, by changing of the direction of the magnetic field to 45° and −45° to the horizontal line, the MNPs were found to form clusters in the

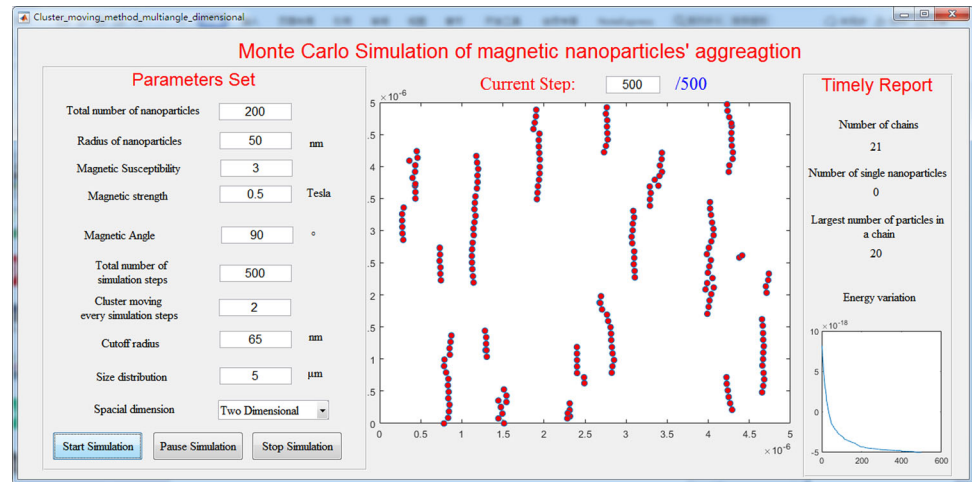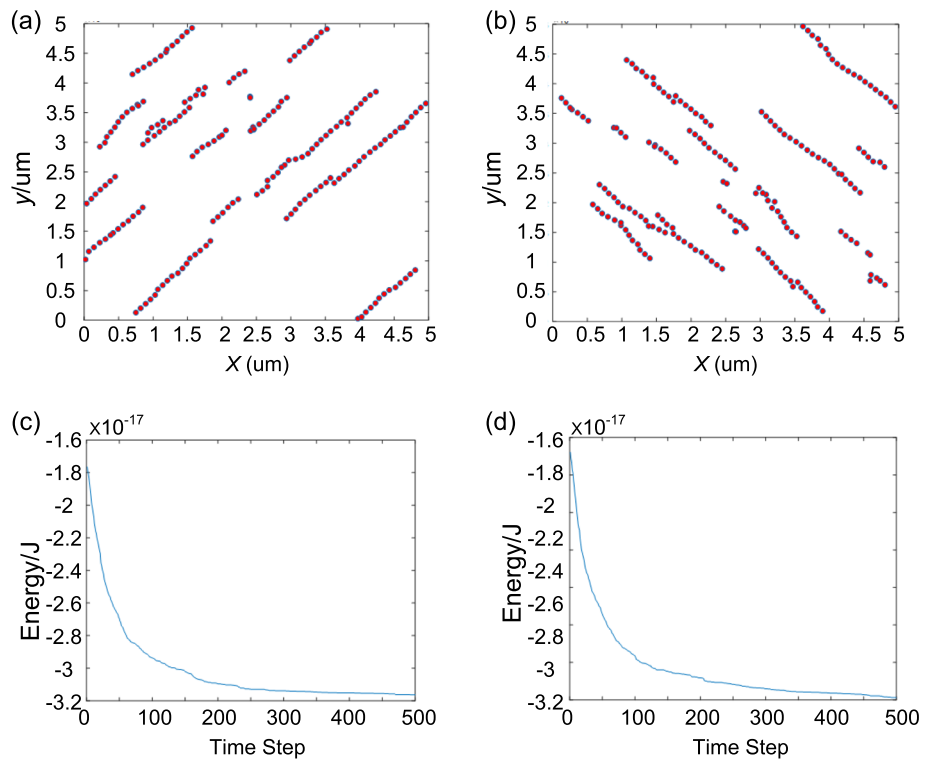**Figure 1** Monte Carlo simulation system of MNPs' aggregation.

Figure 2 The clusters in 45° (**a**) and −45° (**b**) and the total energy variation of the system (**c**) and (**d**).


direction of 45° and −45° shown in Fig. 2. Variation of the system energy corresponding to the two conditions both display a decrease as the increasing steps. Comparing the energy variation, the system energy after 500 steps is not the same because of the difference at the primary. Thus, the primary condition will have an influence on the final results. From the simulation, we also find that the MNPs in the clusters don't always stand absolutely in a line. But a lot of small MNPs will stay beside, which make the clusters not perfectly straight. Therefore, the MNPs

will aggregate to reduce the system energy under an outside static magnetic field.

Cluster rotation and enhanced diffusion

Rotation of the clusters always follows the direction changing of the magnetic field. When there is an angle θ between the direction of the easy magnetization shaft of the cluster and the applied magnetic field, the cluster will be under a magnetic torque. The magnetic torque generally can be given as $\vec{\tau}_F = \vec{m} \times \vec{B}$,

Figure 3 The clusters rotate as the magnetic field.
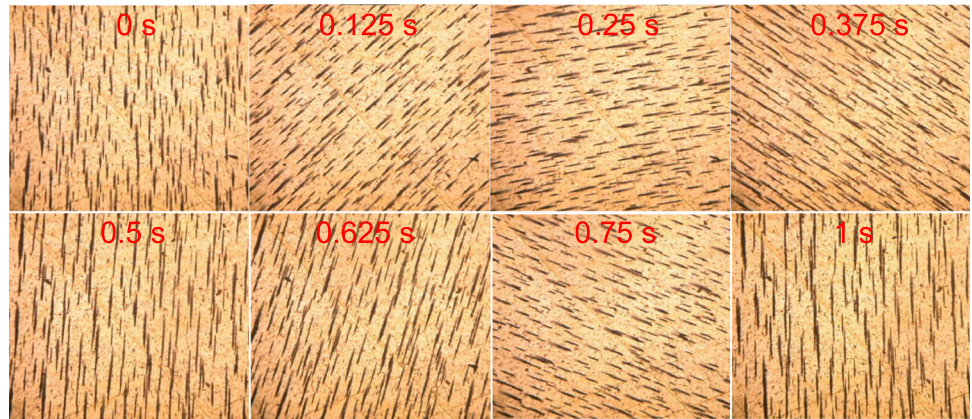
where $\vec{B}$ is the magnetic field, and $\vec{m}$ is the magnetic moment of the clusters. Furthermore, if the cluster rotates at a fluid environment, then there is fluid torque applied on it, as $\vec{\tau}_f = 8\pi\eta R^3 \frac{d\vec{\theta}}{dt}$, which is adapted from the Stokes equation, where η is the kinematic viscosity, and R is the equivalent radius of the aggregation. Then, the motion angular speed of the MNPs cluster can be as follows by neglecting other forces:

$$\frac{d\vec{\theta}}{dt} = \frac{\vec{m} \times \vec{B}}{8\pi\eta R^3}$$

Therefore, when the angle between $\vec{m}$ and $\vec{B}$ is changed, the angular velocity of the clusters will rotate with the direction. Figure 3 shows the clusters rotate as the variation of the magnetic field in xy plane within 1 s. The changing of the magnetic field will help re-direct the clusters.

When a point rotates at a space Ω, there will be a vertex around it and the flow velocity can be modeled as $\vec{u}(\vec{r}) = \nabla \times \frac{\vec{\gamma}}{r} = \frac{\vec{\gamma} \times \vec{r}}{r^3}$, where $\vec{r}$ is the position vector of the point, and $\vec{\gamma}$ represents the characterization of the rotlet. Here, we can let then $\vec{\gamma}$ as the rotational angular velocity of the clusters. Then, the fluid vertex velocity induced by the clusters can be modeled as:

$$\vec{u}(\vec{r}) = \frac{\vec{m} \times \vec{B} \times \vec{r}}{8\pi\eta R^3 r^3}$$

Therefore, the rotating magnetic cluster driven by the rotating magnetic field will induce a rotational velocity around the cluster. The molecular diffusion in the fluid can then be $D = D_f + D_{\vec{u}}$, where D_f is the free diffusion, and $D_{\vec{u}}$ is the diffusion induced by the flow fluid. Therefore, the diffusion can be enhanced by applying the rotation of the MNPs clusters. The rotation can also be accompanied by a translation

Figure 4 The rotation and translation of the clusters under combination of static and rotational magnetic field.
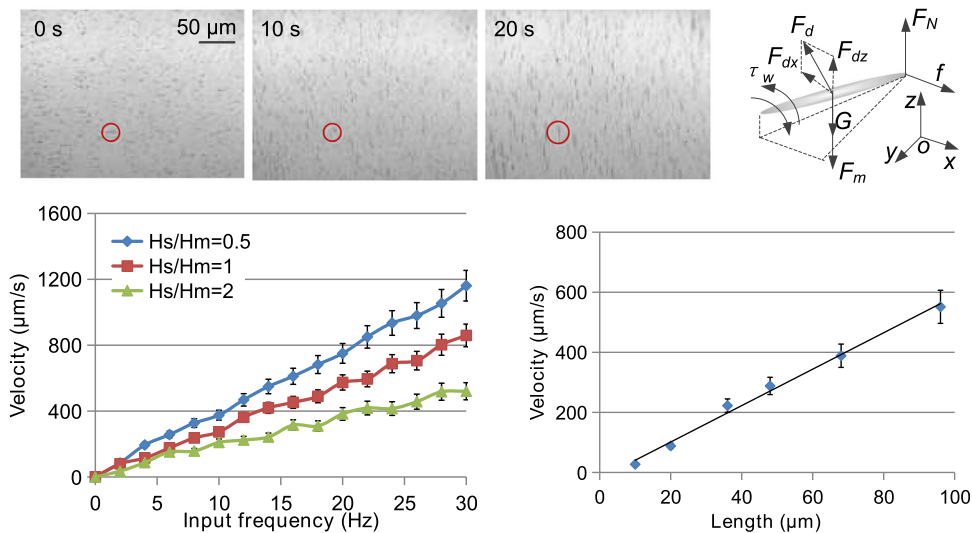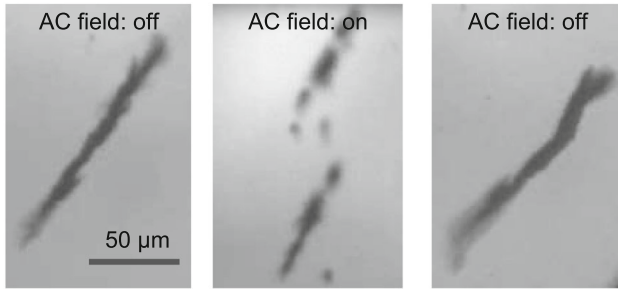
Figure 5 The break-up and re-aggregation of a MNPs cluster.

motion when one end of the aggregation rotates and rubs the plane. The friction force will push the aggregation forward. When considering the magnetic field. The observation is shown in Fig. 4. The static magnetic field and a rotational magnetic field are applied in the direction of x axis and yz axis, respectively. The rod-like clusters rotate with a translation toward the left side during 20 s. The right figure gives the force diagram of a rod-like cluster.

The average translation velocity is measured and is shown in Fig. 3. This shows that the translation velocity is almost linear to the frequency as well the length of the cluster. From the linear relationship, we can know that the translation velocity has a relationship as time t_0:

$$\bar{v} = \frac{2a}{\sqrt{1 + (H_s/H_m)^2}}\left[f - \frac{1}{4\pi t_0}\sin(4\pi f t_0)\right]$$

where a is the length of the cluster. H_s and H_m are static magnetic field and amplitude of the rotating magnetic field. From the equation, we can adjust the ratio of the static and rotating magnetic field to obtain different average velocity of the clusters.

Break-up of clusters

The clusters may also break up during the rotation because of hydrodynamic stresses [27]. Here, we did a research into the break-up of the clusters by improving the frequency of the magnetic field. Figure 5 shows that a complete cluster breaks into pieces when an alternating magnetic field (AC field) with frequency of 50 Hz is on. At primary, the MNPs have aggregated into a complete cluster when a static magnetic field in the 45° is applied. When the AC field is on, the cluster rotates about its easy axis and breaks into two more pieces. However, the broken clusters aggregate again when the AC field is off. This

displays that the clusters can dynamically aggregate and disperse.

The break-up mechanism of the clusters lies in the fact that the cluster is composed of many MNPs, which are connected by the magnetic force. The force between two body has a high-order attenuation relationship with the distance of the MNPs. In the rotational process when the frequency is very high, the fluid moment applied to the clusters will be also very large. When such a force overcomes the magnetic force, the MNPs will escape away from the cluster and result in the disintegration. The re-aggregation of the cluster is observed again and this is as a result of the magnetic attraction because of the static magnetic field. Therefore, breaking up and re-aggregation can be a reversible process by controlling the clusters with alternating magnetic field. This mechanism contributes to strengthening and relaxing the MNPs in an cluster and can be applied in different station.

Deep focusing of MNPs

Focusing MNPs in depth is a challenge for the impossibility for the accumulation of the magnetic induction line at a place far away with only a single magnetic source. Meanwhile, a static magnetic field can't hold a magnetic object far away to stable condition. We adopt a variable magnetic field produced by a group of hollow magnetic coils for the deep focusing process. For one pair of magnetic coils, in which different current is input into the inner and outer coils, the magnetic field in the axis of the coils can be modeled as:

$$H_x(x) = \frac{1}{2}\left[\frac{I_i R_i^2 N_i}{(R_i^2 + x^2)^{3/2}} - \frac{I_o R_o^2 N_o}{(R_o^2 + x^2)^{3/2}}\right]$$

where R_i, R_o are the radius of the inner and outer coil, I_i, I_o are the currents of the inner and outer coil, N_i, N_o are the turns of copper line at the inner and outer coil, x is the distance from the center of the coils. Then, there will be two field free points (FFP). And the displacement can be:

$$x_{\text{FFP}_{1,2}} = \pm\sqrt{\frac{R_o R_i^{4/3} - R_i(N_o I_o R_o^2/N_i I_i)^{2/3}}{\left(\frac{N_o I_o}{N_i I_i}R_i^2\right)^{2/3} - R_o^{4/3}}}$$

Furthermore, we make a COMSOL simulation and observe the magnetic distribution in the region. The

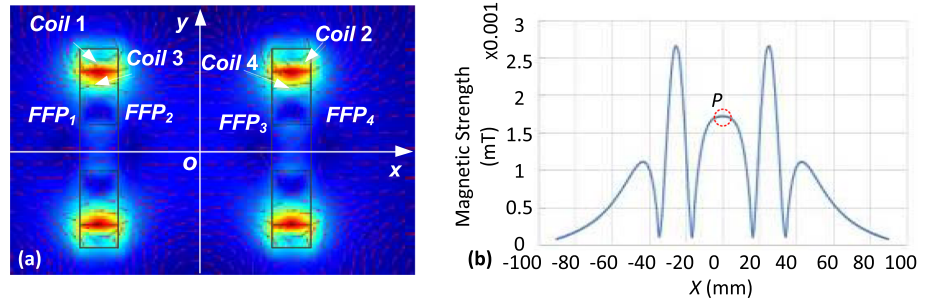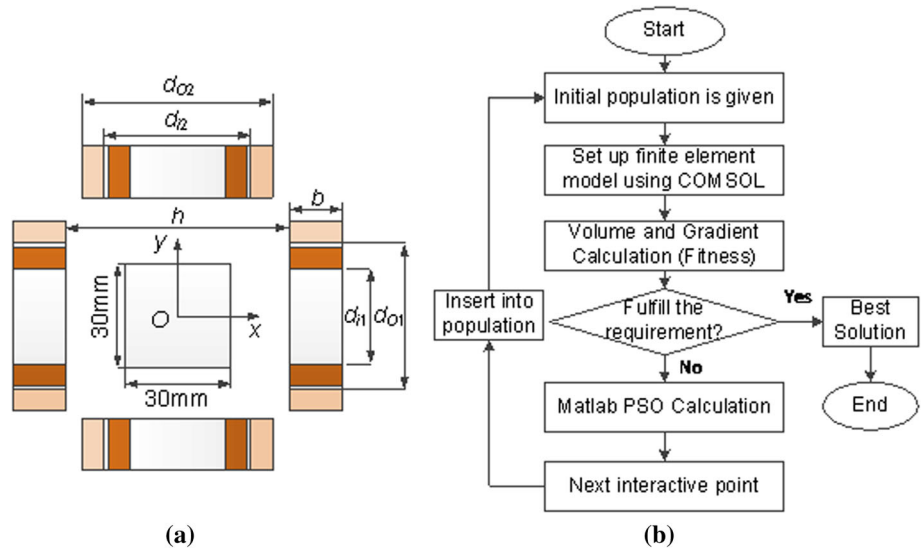**Figure 6** Distribution of magnetic field with two groups of hollow coils.

Figure 7 Coils optimization model (**a**) and the flow chart (**b**).

(a) (b)

analysis of the two group of 4 hollow magnetic coils, in which the currents into them are in different directions as shown in Fig. 6a. The distribution of the magnetic field strength in the axis line of the coil is shown in Fig. 6b. A point with local highest magnetic strength forms at center of the coil system. Four points with local least magnetic strength form as well. As a result, the MNPs among the two FFP will be pushed to the center point. Then, the MNPs can be focused at the place far away from the magnetic sources.

The design of the group of hollow coils is first carried out. According to the symmetry of the system, the coils in the y and z-axis will be set up the

Figure 8 Finding two best points in the PSO algorithm.

same as that in the x-axis. A two-dimensional hollow coil will be designed with optimization method. The objectives for the design are to obtain largest average gradient and minimum volume of the coils. The simulation is a combination COMSOL and MATLAB software. The optimization process is as follows. Primarily, a number of points are random given, and then, a finite element model is set up by using COMSOL. The volume and the magnetic gradient in the simulation region are calculated, which can be known as the fitness. Then, if the fitness fits the requirement, the optimization will be suspended and the result will be seen as the best solution. However, if the fitness doesn't fit the requirement, a new point will be generated and inserted into the population. The objective of generating a new point is on one hand for improving the accumulation efficiency, and on the other hand for the reduction of the energy in the process. The optimization flow model and flow chart are shown in Fig. 7.

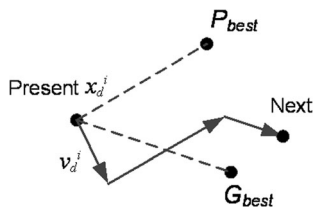The optimization analysis was carried out by using the particle swarm optimization (PSO) algorithm. The

Table 1 The optimization result of the system

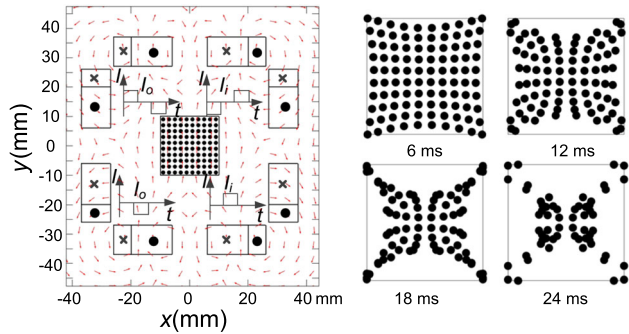| Parameters	d_{O1} (mm)	d_{O2} (mm)	d_{i1} (mm)	d_{i2} (mm)	h (mm)	B (mm)	$I_{i(A)}$	$I_{O(A)}$	Coil volume (mm^3)	Average gradient (A/m^2)
Initial value	60	80	40	60	80	10	1	2	37,691.11	49.497
Optimization	71.23	78.56	38.63	71.23	79.36	10	0.50	2.50	36,751.89	147.002

Figure 9 Focusing MNPs with alternating pulsating currents input into the coils.

basic ideal of the algorithm is to find next new point by looking for two best points, global and local best points. And then, the current point will move toward to the two points with the velocity that is given. The moving velocity of the current point can be given by the following equation:

$$v_d^i(t+1) = \omega v_d^i(t) + (1-r_2)c_1 r_1 (P_{\text{best}\_i} - x_d^i(t)) + (1-r_2)c_2 (1-r_1)(G_{\text{best}\_i} - x_d^i(t))$$

where c_1 and c_2 are two positive constants and the accelerating velocities. r_1 and r_2 are randoms between 0 and 1. P_{best_i} and G_{best_i} are local and global best points. v_d^i is the velocity of the i-th particles. And t is the time in the simulation. The whole process can then be seen in Fig. 8.

The results shown in Table 1 display that the volume of the coils reduces from 37,691.11 to 36,751.89 mm^3. The average gradient in the region is improved from 47.797 to 147.002 A/m^2. The simulation is then carried out with the optimized coils.

The optimized coil group is then used to the accumulate the MNPs. Simulation is carried out in a square area of 30 mm × 30 mm, where 100 MNPs at the nodes of the grids are primarily generated uniformly. The other parameters are shown as: the magnetic susceptibility 5 and radius 50 nm. The turns of the magnetic coils are 300 with a diameter of the copper line 1 mm. The pulsating current input into the electromagnetic coils sequentially is an alternating pulsating current with frequency of 100 Hz. Figure 9 shows that the primary dispersed MNPs are found to focus at the center after about 30 ms. The shaping outline of the accumulating MNPs displays an arc curve, which is induced by the magnetic timely distribution. The MNPs close to the center will move with a fast speed and accumulate at the place much more quickly. However, the MNPs in the angle of 45 degree move with a lowest speed. Thus, the accumulation of the MNPs in that angle will not be obvious. Aggregation mainly occurs with the MNPs that are close to the central axis of the coils.

The accumulation of MNPs in the position far away from the origin of the magnet has been realized, and the sizes of coils are optimized for the designation.

Accumulation and thrombolysis experiments

An experimental device for thrombolysis was set up and is shown in Fig. 10. A magnetic control system contains six groups of inner and outer coils, which were designed according to the optimized sizes. A microfluidic channel was used for the mimic microvessel in which the thrombus was inserted first by using a pipette. The pulsating currents were input into the coils in the y- and z-axis by using a digital current generator. The x-axis was input an alternating current with sine wave of the same frequency. The CCD recorded the boundary motion of the thrombus in the channel, and the average moving speed could be calculated by dividing the time with the boundary moving distance.

The experiment of focusing Fe$_3$O$_4$ MNPs in a place far away from the magnet source was first carried out. A plastic pipe with diameter of 10 mm was used for the 3D space containing the MNPs fluid. Then the pulsating currents with a frequency of 100 Hz were input into the xyz axis coils sequentially. Figure 11 shows that the primary dispersed MNPs suddenly

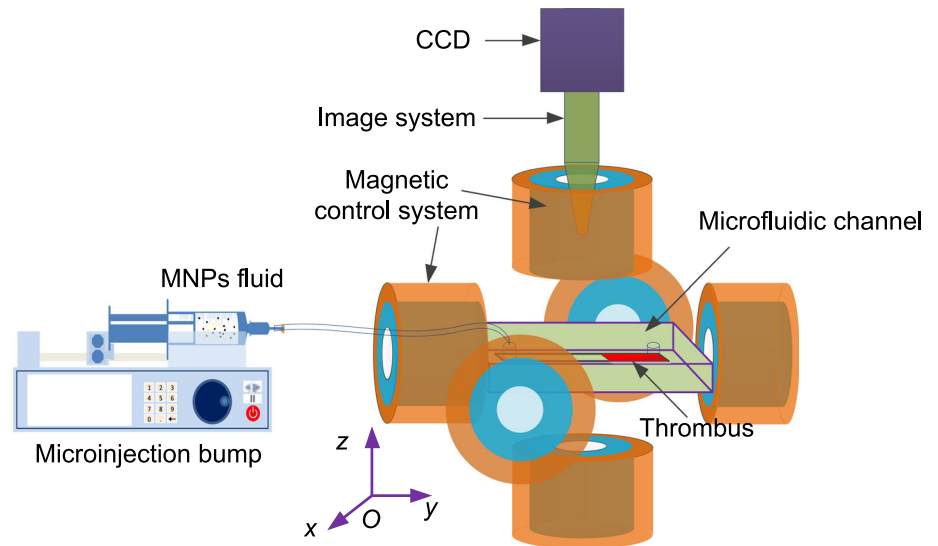**Figure 10** In vitro thrombolysis experimental device.

Figure 11 The accumulation of MNPs in the center of the pipe.

accumulated in the center of the pipe. However, because the process was very fast, the final and primary conditions of the MNPs were recorded. This experiment only displayed the primary and final condition of the MNPs in the fluid. However, the aggregation of MNPs descended at the bottom of the pipe because of the large gravity. This coincides with the theoretical simulation process. Thus, the designed coil system could give a good performance on the accumulation of the MNPs in a place far away from the magnet source.

Then, thrombolysis with accumulated urokinase-coated MNPs and pure urokinase under alternating magnetic field was carried out. In this experiment, 10 mg/ml MNPs solution and 50 µg/ml pure urokinase were inserted into the channel by a micro-fluid bump. At first, a pulsating current was input into the x- and z-axis coils to focus the MNPs and a DC current was input into the y-axis coil to produce a static magnetic field. Then, an alternating current with 50 Hz was input into the x- and z-axis coils to produce a rotating magnetic field. The motion of thrombus boundary, representing the lysis of the thrombus, was recorded by applying MNPs and pure urokinase, respectively. The results showed that when applying 50 µg/ml pure urokinase, the boundary motion velocity was about 20 µm/s. The velocity was increased to 45 µm/s when 10 mg/ml MNPs were applied. This implies that the lysis

Figure 12 The rotating cluster impacts on the thrombus and breaks the thrombus.
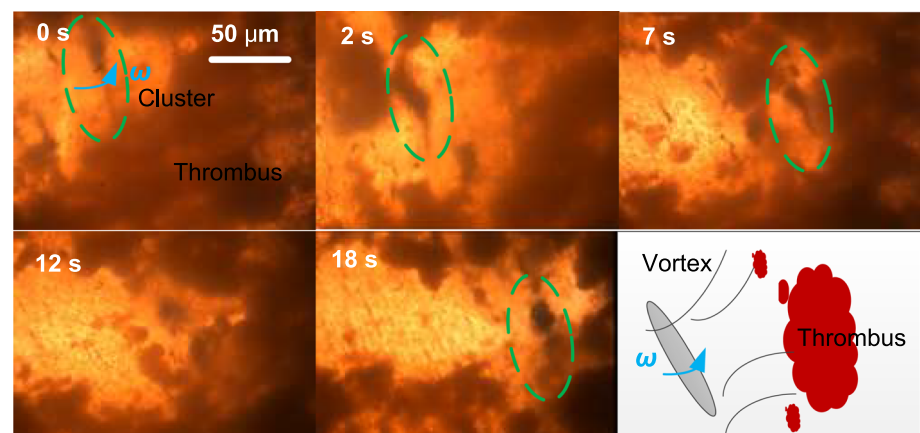
velocity was promoted to 2 more times than the pure urokinase.

To observe the phenomenon more closely, a 50 × microlens was used to record the micro-motion of the clusters. At 0 s, the DC current of 2 A was input into the y-axis coil to induced a static magnetic field, which magnetized the NPs in the solution. Then, a pulsating current was input into the x- and z-axis coil, and the magnetized NPs were focused at the boundary of the thrombus and form elongated clusters. Then, AC current with amplification of 2 A and frequency of 50 Hz was input into the x and z-axis coils. The clusters rotates fast as the produced rotating magnetic field, shown in Fig. 12. The figures display that during 18 s, the clusters hit the thrombus seriously as well as inducing a strong vortex near the thrombus to break the thrombus. Thus, by applying rotating magnetic field, the clusters would have a great impact on the target. Though it only broke the thrombus into little piece and was considered as a incomplete thrombolysis, it might also help further improve the thrombolysis for the increasing of the area contacting the urokinase.

Results and discussion

The formation of clusters under magnetic field has been simulated with MATLAB. Through combining the PSO algorithm with cluster-moving method, clusters with different lengths have been found in the simulation. The mechanism of forming rod-like clusters is due to the energy reduction of the system. The system is seeking for a equilibrium point to remain a low energy situation. The cluster-moving method overcomes the disadvantages in previous research that once a cluster formed, they will not move any more. Thus, more larger clusters may not be obtained. This is because the Lennard–Jones potential has an inverse square proportional to the distance between the two NPs. As a result, the two closest NPs will determine whether the NPs can move or not. Thus, the small chains can no longer move to form larger ones. Cluster-moving method can result in the accuracy of the simulation process.

The group of hollow magnetic coils is designed and the strategy to accumulate the MNPs far away from the magnet source through current control is put forward. By applying an asymmetric alternating pulsating current into the coils, the MNPs can be focused in a position deviated from the central place. The accumulation action is considered as a promotion of the concentration of the thrombotic which is conjugated on the surface of the MNPs. The thrombolysis rate can then be improved for more thrombotic molecular contacting the thrombus. The experiments have shown thrombolysis efficiency is improved to two more with the focusing and rotating. Therefore, when the thrombus locates at the deep vein of the body, guidance of the MNPs to such a place with non-contact control will be of great importance. The thrombolysis can further be improved by the rotational motion for the enhancement of the diffusion of the thrombotic in the fluid to the surface of the thrombus. In the experiment, the urokinase-coated MNPs are adopted and for the. In fact, though they are not connected, the MNPs clusters can also enhance the diffusion to help the urokinase reach the thrombus quickly.

From the research, the breaking of the clusters can also be controlled by improving the rotational frequency of the magnetic field. The clusters are considered to break because of the promotion of the fluid resistance and centrifugal force when a rotational motion is improved. The outside force overcomes the attraction force and breaks the clusters into pieces. Such an action will help reduce the possibility of occluding the microvessels after thrombolysis. Since from the experiment, we also observe that many clusters also hit the thrombus. Therefore, we can let the MNPs in the fluid form large clusters, which may help apply a larger hit force on the thrombus to break it, because of the inertial force with a larger mass of the clusters. After the process, the magnetic frequency can be improved for a damage effect on the cluster. However, the unavoidable aggregation of the clusters during the guidance may also result in the risk of blocking the vessels. Controlling the size of the clusters at any time is also an importance research.

For urokinase-coated MNPs, they are synthesized as the way shown in our former published work [25]. The prepared MNPs have good biocompatibility. Moreover, Naumenko et al. reported that iron oxide NPs can be eliminated from the body through the physiological metabolism [28]. Compared with the reported thrombolysis studies, the advantage of the strategy lies in the fact of quickly focusing the MNPs in the deep lesion to improve the amount of the drugs far away from the magnetic source. Meanwhile, by driving the MNPs to rotate, the clusters can induce

vortex or hit directly to break the thrombus. As a result, the thrombolysis efficiency can be improved. This can be a good alternative for the future clinical use.

Conclusions

We have demonstrated that focusing and rotating MNPs clusters can effectively improve the thrombolysis rate to 2 more times. A coil system consisting of six groups of inner and outer hollow axial coils was designed with the PSO algorithm for the manipulation. For fast accumulation of the MNPs, a current strategy was adopted by using the combination of alternating pulsating current and alternating current. Controlling the aggregation and disintegration of the clusters was researched by improving or decreasing the frequency of the alternating magnetic field. The manipulation system could be an effective solution for the thrombolysis enhancing in future clinical use.

Acknowledgements

Data and code availability

The code can be obtained from the correspondence.

Declarations

Conflict of interest The authors declare no conflict of interest.

Ethical approval Not applicable.

References

[1] https://www.who.int/data/gho/data/themes/mortality-and-global-health-estimates

[2] Pitek AS, Park J, Wang Y, Gao H, Hu H, Simon DI, Steinmetz NF (2018) Delivery of thrombolytic therapy using rod-shaped plant viral nanoparticles decreases the risk of hemorrhage. Nanoscale 10:16547–16555. https://doi.org/10.1039/C8NR02861C

[3] Furie B, Furie BC (2008) Mechanisms of thrombus formation. New Engl J Med 359:938–949. https://doi.org/10.1056/NEJMra0801082

[4] Prilepskii AY, Fakhardo AF, Drozdov AS, Vinogradov VV, Dudanov IP, Shtil AA, Bel'Tyukov PP, Shibeko AM, Koltsova EM, Nechipurenko DY (2018) Urokinase-conjugated magnetite nanoparticles as a promising drug delivery system for targeted thrombolysis: synthesis and preclinical evaluation. ACS Appl Mater Inter 10:36764–36775. https://doi.org/10.1021/acsami.8b14790

[5] Jørgensen NP, Zobek N, Dreier C, Haaber J, Ingmer H, Larsen OH, Meyer RL (2016) Streptokinase treatment reverses biofilm-associated antibiotic resistance in staphylococcus aureus. Microorganisms 4:36. https://doi.org/10.3390/microorganisms4030036

[6] Chapurina YE, Drozdov AS, Popov I, Vinogradov VV, Dudanov IP, Vinogradov VV (2016) Streptokinase@ alumina nanoparticles as a promising thrombolytic colloid with prolonged action. J Mater Chem B 4:5921–5928. https://doi.org/10.3390/microorganisms4030036

[7] Lee CD, Folsom AR, Blair SN (2003) Physical activity and stroke risk: a meta-analysis. Stroke 34:2475–2481. https://doi.org/10.1097/00005768-200305001-00375

[8] Strong K, Mathers C, Bonita R (2007) Preventing stroke: saving lives around the world. Lancet Neurol 6:182–187. https://doi.org/10.1016/S1474-4422(07)70031-5

[9] Chung TW, Wang SS, Tsai WJ (2008) Accelerating thrombolysis with chitosan-coated plasminogen activators encapsulated in poly-(lactide-co-glycolide)(PLGA) nanoparticles. Biomaterials 29:228–237. https://doi.org/10.1016/j.biomaterials.2007.09.027

[10] Raabe RD (2010) Ultrasound-accelerated thrombolysis in arterial and venous peripheral occlusions: fibrinogen level effects. J Vasc Interv Radiol 21:1165–1172. https://doi.org/10.1016/j.jvir.2010.03.020

[11] Zenitani T, Suzuki R, Maruyama K, Furuhata H (2008) Accelerating effects of ultrasonic thrombolysis with bubble liposomes 35:5–10. https://doi.org/10.1007/s10396-007-0163-x

[12] Lanza G, Marsh J, Scott M, Schmieder A, Caruthers S, Pan D, Wickline S (2010) Rationale for a nanomedicine approach to thrombolytic therapy. Stroke 41:S42–S44. https://doi.org/10.1161/strokeaha.110.598656

[13] Feng B, Zhang J, Su Y, Tang YC, Liu JN (2009) Chemical conjugation of urokinase to magnetic nanoparticles for targeted thrombolysis. Biomaterials 30:5125–5130. https://doi.org/10.1016/j.biomaterials.2009.06.006

[14] Chen JP, Liu CH, Hsu HL, Wu T, Lu YJ, Ma YH (2016) Magnetically controlled release of recombinant tissue plasminogen activator from chitosan nanocomposites for

targeted thrombolysis. J Mater Chem B 4:2578–2590. https://doi.org/10.1039/C5TB02579F

[15] Kumar S, Jana AK, Dhamija I, Singla Y, Maiti M (2013) Preparation, characterization and targeted delivery of serra-tiopeptidase immobilized on amino-functionalized magnetic nanoparticles. Eur J Pharm Biopharm 85:413–426. https://doi.org/10.1016/j.ejpb.2013.06.019

[16] Roseita E, Donald A, Tomalia (2001) Poly(amidoamine) (PAMAM) dendrimers: from biomimicry to drug delivery and biomedical applications. Drug Discov Today 6:427–436. https://doi.org/10.1016/s1359-6446(01)01757-3

[17] Mora-Huertas CE, Fessi H, Elaissari A (2010) Polymer-based nanocapsules for drug delivery. Int J Pharmaceut 385:113–142. https://doi.org/10.1016/j.ijpharm.2009.10.018

[18] Moerland CP, Van IJzendoorn LJ, Prins MWJ (2019) Rotating magnetic particles for lab-on-chip applications–a comprehensive review. Lab Chip 19(6):919–933. https://doi.org/10.1039/C8LC01323C

[19] Perera AS, Zhang S, Homer-Vanniasinkam S, Coppens MO, Edirisinghe M (2018) Polymer–magnetic composite fibers for remote-controlled drug release. ACS Appl Mater Inter 10:15524–15531. https://doi.org/10.1021/acsami.8b04774

[20] Zhou J, Guo D, Zhang Y, Wu W, Ran H, Wang Z (2014) ACS Appl Mater Inter 6:5566–5576. https://doi.org/10.1021/am406008k

[21] Alexiou C, Jurgons R, Schmid R, Erhardt W, Parak F, Bergemann C, Iro H (2005) Magnetic drug targeting–a new approach in locoregional tumor therapy with chemothera-peutic agents. Exp Anim Stud Hno 53:618–622. https://doi.org/10.1007/s00106-004-1146-5

[22] Torno MD, Kaminski MD, Xie Y, Meyers RE, Mertz CJ, Liu X, O'Brien WD Jr, Rosengart AJ (2008) Improvement of in vitro thrombolysis employing magnetically-guided microspheres. Thromb Res 121:811. https://doi.org/10.1016/j.thromres.2007.08.017

[23] Labinac V, Erceg N, Kotnik-Karuza D (2006) Magnetic field of a cylindrical coil. AM J Phys 74:621–627. https://doi.org/10.1119/1.2198885

[24] Gou X, Yang Y, Zheng X (2004) Analytic expression of magnetic field distribution of rectangular permanent mag-nets. Appl Math Mech 25:297–306. https://doi.org/10.1007/bf02437333

[25] Li Q, Liu X, Lu Z, Yang W, Lei Z, Chang M (2019) Con-jugation of Urokinase to water-soluble magnetic nanoparti-cles for enhanced thrombolysis. Appl Sci 9:4862. https://doi.org/10.3390/app9224862

[26] Andreu JS, Camacho J, Faraudo J (2011) Aggregation of superparamagnetic colloids in magnetic fields: the quest for the equilibrium state. Soft Matter 7:2336–2339. https://doi.org/10.1039/C0SM01424A

[27] Bałdyga J, Orciuch W, Makowski Ł, Malski-Brodzicki M, Malik K (2007) Break up of nano-particle clusters in high-shear devices. Chem Eng Process 46:851–861. https://doi.org/10.1016/j.cep.2007.05.016

[28] Naumenko V, Nikitin A, Kapitanova K, Melnikov P, Majouga A (2019) Intravital microscopy reveals a novel mechanism of nanoparticles excretion in kidney[J]. J Control Release 307:368–378. https://doi.org/10.1016/j.jconrel.2019.06.026